◆ Human Brain Mapping 38:5128–5140 (2017) ◆

Oscillations During Observations: Dynamic Oscillatory Networks Serving Visuospatial Attention

Alex I. Wiesman,[1,2] **Elizabeth Heinrichs-Graham**,[1,2] **Amy L. Proskovec**,[1,3] **Timothy J. McDermott**,[1,2] **and Tony W. Wilson**[1,2]*

[1]*Center for Magnetoencephalography, University of Nebraska Medical Center, Omaha, Nebraska*
[2]*Department of Neurological Sciences, University of Nebraska Medical Center, Omaha, Nebraska*
[3]*Department of Psychology, University of Nebraska, Omaha, Nebraska*

Abstract: The dynamic allocation of neural resources to discrete features within a visual scene enables us to react quickly and accurately to salient environmental circumstances. A network of bilateral cortical regions is known to subserve such visuospatial attention functions; however the oscillatory and functional connectivity dynamics of information coding within this network are not fully understood. Particularly, the coding of information within prototypical attention-network hubs and the subsecond functional connections formed between these hubs have not been adequately characterized. Herein, we use the precise temporal resolution of magnetoencephalography (MEG) to define spectrally specific functional nodes and connections that underlie the deployment of attention in visual space. Twenty-three healthy young adults completed a visuospatial discrimination task designed to elicit multispectral activity in visual cortex during MEG, and the resulting data were preprocessed and reconstructed in the time–frequency domain. Oscillatory responses were projected to the cortical surface using a beamformer, and time series were extracted from peak voxels to examine their temporal evolution. Dynamic functional connectivity was then computed between nodes within each frequency band of interest. We find that visual attention network nodes are defined functionally by oscillatory frequency, that the allocation of attention to the visual space dynamically modulates functional connectivity between these regions on a millisecond timescale, and that these modulations significantly correlate with performance on a spatial discrimination task. We conclude that functional hubs underlying visuospatial attention are segregated not only anatomically but also by oscillatory frequency, and importantly that these oscillatory signatures promote dynamic communication between these hubs. *Hum Brain Mapp 38:5128–5140, 2017.*

Additional Supporting Information may be found in the online version of this article.

Contract grant sponsor: NIH; Contract grant number: R01 MH103220; Contract grant sponsor: NSF; Contract grant number: #1539067; Contract grant sponsor: University of Nebraska Medical Center's Research Support Fund

*Correspondence to: Tony W. Wilson, Center for Magnetoencephalography, 988422 Nebraska Medical Center, Omaha, NE 68198-8422, USA. E-mail: twwilson@unmc.edu

Received for publication 5 June 2017; Accepted 26 June 2017.
DOI: 10.1002/hbm.23720
Published online 17 July 2017 in Wiley Online Library (wileyonlinelibrary.com).

Key words: cortical oscillations; MEG; phase coherence; visual attention

INTRODUCTION

Visuospatial attention is central to basic cognitive function. With the complexity inherent in most visual scenes, the ability to direct cognitive resources toward discrete features, properties, or groupings of external stimuli within the scene is paramount for rapid analysis and reaction to salient environmental pressures. Neuroimaging and lesion studies have indicated a widespread network of functional nodes is involved in visuospatial attention, including hubs in frontal, parietal, and visual cortices [Corbetta and Shulman, 2002; Desimone and Duncan, 1995; Maris and Oostenveld, 2007; Posner and Petersen, 1990]. Although the time course of neural activity in these regions during attention allocation and processing has been a topic of major interest for decades, much remains to be discovered and this is especially true for the network level dynamics. Early studies of patients with attentional neglect found that lesions of superior parietal cortex corresponded to deficits in the contralateral visual hemifield [Posner et al., 1984], and microelectrode recordings in nonhuman primates discovered that attention-related activity in these regions tended to occur roughly 80–100 ms poststimulus [Lynch et al., 1977]. Later studies in humans found that visuospatial attention significantly modulated neural activity in the bilateral superior parietal lobule between 120 and 180 ms [Di Russo et al., 2003]. In extrastriate cortices, attention to visual stimuli has been found to enhance the power of event-related potentials as early as 80–90 ms [Di Russo et al., 2003; Noesselt et al., 2002], with sustained activity persisting in primary visual cortex between 140 and 250 ms [Noesselt et al., 2002]. Interestingly, the time course of attention-related neural activity in the frontal cortices appears to be much more variable, but this is likely attributable to variations in the cognitive task (e.g., task switching and distractor suppression) and the extent of executive functions that were required for task execution. Importantly, no studies to date have quantified the time series of all attention nodes in parallel within a single experiment, making it difficult to surmise the temporal interrelationships between nodes, and the temporal progression of activity through the circuitry and its association with visuospatial attention processes.

Recently, interest has surged in uncovering the mechanisms by which neural networks encode and decode information through the use of carrier frequencies, oscillations, cross-frequency coupling, and other coding schemes [Buzsaki and Draguhn, 2004; Schnitzler and Gross, 2005]. A number of the classical frequency bands, including theta (4–7 Hz), alpha (8–14 Hz), beta (14–30 Hz), and gamma (30 Hz+), have been associated with performance on attention-demanding tasks in humans. For example, numerous studies have implicated theta oscillations as a vital coding scheme for the temporal organization of visual attention sampling and processing [Busch et al., 2009; Jensen and Tesche, 2002; Landau and Fries, 2012; Landau et al., 2015; Verbruggen et al., 2010]. Synchronization in the alpha band has been shown to index the inhibition of incoming visual information in the occipital cortices [Handel et al., 2011; Spaak et al., 2014]. Furthermore, beta suppression in the parietal lobes has been associated with local neural processing [Rosanova et al., 2009], while long-range phase synchronization in the beta range has been shown to covary with target detection on an attentional blink task [Gross et al., 2004], and is deficient in patients with attentional neglect of one hemifield [He et al., 2007]. Finally, gamma activity in the visual cortices is modulated by attention allocation [Doesburg et al., 2008; Edden et al., 2009; Tallon-Baudry et al., 2005; Vidal et al., 2006], particularly by top–down signals from frontal regions that are also implicated in attention [Baldauf and Desimone, 2014; Doesburg et al., 2008; Marshall et al., 2015]. These experiments collectively suggest that attention allocation and processing relies on a broad range of quasi-, regionally-, and functionally-specific oscillatory frequencies for the processing and transmission of task-relevant information.

Engagement of attention has also been found to modulate functional connectivity (FC) between the aforementioned functional hubs [Baldauf and Desimone, 2014; Buchel and Friston, 1997; Doesburg et al., 2008; He et al., 2007; Saalmann et al., 2007; Siegel et al., 2008; Szczepanski et al., 2014]. However, limited temporal resolution has precluded many of these studies from examining the dynamics of FC changes on a fine temporal scale, which is problematic as several studies have shown that functional coupling between brain regions can strongly fluctuate on a subsecond timescale [David et al., 2005; Heinrichs-Graham and Wilson, 2015a; Honey et al., 2007; Rissman et al., 2004; Valencia et al., 2008; Wiesman et al., 2017, 2016], and that these dynamics are often predictive of associated neural and behavioral responses. Moreover, such coupling can be frequency-specific and/or multispectral, and may provide critical bandwidth for communication between attention-related regions with shared schemes of information coding (i.e., FC between distant attention regions within the same frequency band), but the interregional dynamics remain to be clarified.

In this study, we adopt a data-driven approach to investigate the neural oscillations and dynamic FC that underlies the allocation of attention to specific stimuli in visual space. To this end, we utilized the millisecond temporal

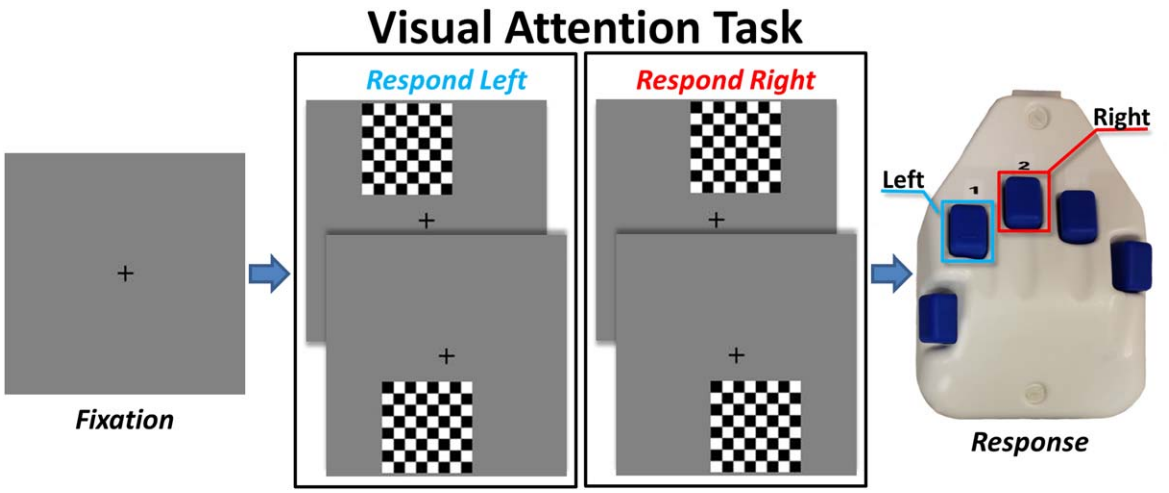

Figure 1.

Visuospatial discrimination paradigm (VisAttend). Each trial was composed of two periods: (**a**) a fixation period lasting about 2000 ms (variable ISI: 1900–2100 ms), 400 ms of which functioned as the baseline, and (**b**) a stimulus-presentation period lasting 800 ms and consisting of the appearance of a checkered grid in one of four locations. Participants were required to indicate by button press the laterality (left or right) of the stimulus position relative to the fixation point. [Color figure can be viewed at wileyonlinelibrary.com]

resolution of magnetoencephalography (MEG), in combination with advanced time–frequency, beamforming, and FC methodologies. We used a novel visuospatial discrimination task and examined the subsecond interval following the presentation of the visual stimulus, but before the participant's response, so as to focus on the neuronal dynamics serving the deployment of attention to the visual space. We hypothesized that common attention-network nodes in the frontal, parietal, and visual cortices would be engaged upon stimulus onset, and that transient increases in frequency-specific FC would emerge among these networks, representing dynamic interregional communication on a subsecond timescale.

MATERIALS AND METHODS

Participants

We enrolled 23 healthy adults (20 right-handed; 13 males) for the study. All participants were between the ages of 22 and 45 (mean = 33.04; SD = 7.23). Exclusionary criteria included any medical illness affecting CNS function (e.g., HIV/AIDS), any neurological disorder, history of head trauma, and current substance abuse. The Institutional Review Board at the University of Nebraska Medical Center reviewed and approved this investigation. Written informed consent was obtained from each participant following detailed description of the study.

Experimental Paradigm

The paradigm used was a novel visuospatial discrimination task, termed *Vis-Attend* (Figure 1). During this task, the participants were seated in a magnetically shielded room and told to fixate on a crosshair presented centrally. After a variable ISI (range: 1900–2100 ms), an 8 × 8 grid was presented for 800 ms at one of the four positions relative to the fixation: above right, below right, above left, or below and to the left (Figure 1). The left/right orientations were defined as a lateral offset of 75% of the grid from the center of fixation. Before the task began, participants were instructed to respond via button press with their right hand whether the grid was positioned to the left (index finger) or right (middle finger) of the fixation point upon presentation of the grid. Each participant performed 240 repetitions of the task concurrent with MEG recording.

MEG Data Acquisition

All recordings were conducted in a one-layer magnetically shielded room with active shielding engaged for environmental noise compensation. With an acquisition bandwidth of 0.1–330 Hz, neuromagnetic responses were sampled continuously at 1 kHz using an Elekta MEG system (Helsinki, Finland) with 306 sensors, including 204 planar gradiometers and 102 magnetometers. During data acquisition, participants were monitored via real-time audio–video feeds from inside the shielded room. Each MEG dataset was individually corrected for head motion and subjected to noise reduction using the signal space separation method with a temporal extension [Taulu and Simola, 2006].

Structural MRI Processing and MEG Coregistration

Prior to MEG measurement, four coils were attached to the subject's head and localized, together with the three

fiducial points and scalp surface, with a 3-D digitizer (Fastrak 3SF0002, Polhemus Navigator Sciences, Colchester, VT, USA). Once the subject was positioned for MEG recording, an electric current with a unique frequency label (e.g., 322 Hz) was fed to each of the coils. This induced a measurable magnetic field and allowed each coil to be localized in reference to the sensors throughout the recording session. As coil locations were also known in head coordinates, all MEG measurements could be transformed into a common coordinate system. With this coordinate system, each participant's MEG data were coregistered with structural T1-weighted MRI data prior to source space analyses using BESA MRI (Version 2.0). Structural MRI data were aligned parallel to the anterior and posterior commissures and transformed into standardized space. Following source analysis (i.e., beamforming), each subject's 4.0 × 4.0 × 4.0 mm functional images were also transformed into standardized space using the transform that was previously applied to the structural MRI volume and spatially resampled.

MEG Preprocessing, Time–Frequency Transformation, and Sensor-Level Statistics

Cardiac artifacts were removed from the data using signal-space projection (SSP), which was accounted for during source reconstruction [Uusitalo and Ilmoniemi, 1997]. The continuous magnetic time series was divided into epochs of 2700 ms duration, with the baseline being defined as −460 to −60 ms before initial stimulus onset. Of note, we shifted our baseline away from the period immediately preceding stimulus onset to eliminate potential contamination by any anticipatory responses. Epochs containing artifacts were rejected based on a fixed threshold method, supplemented with visual inspection. An average of 216.23 (SD = 10.06) trials per participant were used for further analysis.

Artifact-free epochs were transformed into the time–frequency domain using complex demodulation, which involves filtering the complex signal into a number of frequency bands of a predetermined width and overall range (e.g., 2 Hz bands from 2 to 50 Hz), and calculating the power within each band across each successive temporal window [Bingham et al., 1967; Hoechstetter et al., 2004; Papp and Ktonas, 1977]. By decomposing the sensor-level recordings in this way, it is possible to examine the multispectral neural responses underlying performance of a task, which have been suggested to code distinct components of cognition in the human brain [Hari and Salmelin, 1997; Jensen et al., 2014; Roux and Uhlhaas, 2014]. The resulting spectral power estimations per sensor were averaged over trials to generate time–frequency plots of mean spectral density. These sensor-level data were normalized by dividing the power value of each time–frequency bin by the respective bin's baseline power, which was calculated as the mean power during the −460 to −60 ms time period. The specific time–frequency windows used for imaging were determined by statistical analysis of the sensor-level spectrograms across the entire array of gradiometers. Each data point in the spectrogram was initially evaluated using a mass univariate approach based on the general linear model. To reduce the risk of false positive results while maintaining reasonable sensitivity, a two-stage procedure was followed to control for Type 1 error. In the first stage, one-sample t tests were conducted on each data point and the output spectrogram of t values was thresholded at $P < 0.05$ to define time–frequency bins containing potentially significant oscillatory deviations across all participants. In stage two, time–frequency bins that survived the threshold were clustered with temporally and/or spectrally neighboring bins that were also above the threshold ($P < 0.05$), and a cluster value was derived by summing all the t values of all data points in the cluster. Nonparametric permutation testing was then used to derive a distribution of cluster values and the significance level of the observed clusters (from stage one) were tested directly using this distribution [Ernst, 2004; Maris and Oostenveld, 2007]. For each comparison, at least 10,000 permutations were computed to build a distribution of cluster values. Based on these analyses, the time–frequency windows that contained significant oscillatory events across all participants were subjected to a beamforming analysis. Importantly, we performed further analysis only on those significant events that fell within the time window between onset of the visual stimulus and the mean RT across all participants, so as to focus only on activations underlying visuospatial attention and discrimination, rather than other processes inherent to the later portions of our task (i.e., motor termination, response/error-checking, etc.).

MEG Source Imaging and Statistics

MEG preprocessing and imaging used the Brain Electrical Source Analysis (BESA version 6.0) software. Cortical networks were imaged through an extension of the linearly constrained minimum variance vector beamformer [Gross et al., 2001], which employs spatial filters in the time–frequency domain to calculate source power for the entire brain volume. The single images are derived from the cross-spectral densities of all combinations of MEG gradiometers averaged over the time–frequency range of interest. In principle, the beamformer operator generates a spatial filter that passes signals without attenuation from a region of interest, while suppressing activity in all other brain areas. The filter properties arise from the forward solution (lead field) for each location on a volumetric grid specified by input voxel space, and from the MEG covariance matrix. Basically, for each voxel, a set of beamformer weights is determined, which amounts to each MEG sensor being allocated a sensitivity weighting for activity in the particular voxel. This set of beamformer weights is the

spatial filter unique to the given voxel and this procedure is iterated until such a filter is computed for each voxel in the brain. Activity in each voxel is then determined independently and sequentially to produce a volumetric map of electrical activity with relatively high spatial resolution. In short, this method outputs a power value for each voxel in the brain, determined by a weighted combination of sensor-level time–frequency activity. Following convention, we computed noise-normalized source power per voxel in each participant using active (i.e., task) and passive (i.e., baseline) periods of equal duration and bandwidth. Such images are typically referred to as pseudo-*t* maps, with units (pseudo-*t*) that reflect noise-normalized power differences (i.e., active vs passive) per voxel. Grand averages and one-sample *t* tests were then computed using the pseudo-*t* maps from all participants. For all one-sample *t*-test images, a stringent cutoff of $P < 5 \times 10^{-6}$ was utilized to emphasize only the most robust task-related responses. Virtual sensors were computed from the peak voxel of each cluster, which was defined as the voxel with the maximum activation value within each spatially defined cluster. To compute the virtual sensors, we applied the sensor-weighting matrix derived through the forward computation to the preprocessed signal vector, which yielded a time series for the specific coordinate in source space. Note that this virtual sensor extraction was done per participant individually, once the coordinates of interest were known.

Functional Connectivity Analyses

To evaluate dynamic connectivity between attention-related neural regions, we computed phase coherence within the respective frequency bands of our statistically defined clusters. Of note, we only computed phase coherence between the clusters defined from the one-sample *t*-test images. To compute phase coherence, we extracted the phase-locking value (PLV) using the method described by Lachaux et al. [1999]. The virtual sensor signals were band-pass filtered at ±1.0 Hz, and their convolution was computed using a complex Gabor wavelet centered at the target frequency. We extracted the phase of the convolution for each time-frequency bin per trial, and then evaluated the phase relationship between each pair of brain regions across trials to derive the PLV. The PLV reflects the intertrial variability of the phase relationship between pairs of brain regions as a function of time. Values close to 1 indicate strong synchronicity (i.e., phase locking) between the two voxel time series' within the specific time–frequency bin across trials, whereas values close to 0 indicate substantial phase variation between the two signals, and thus, low synchronicity (connectivity) between the two regions. To examine alterations in connectivity following the onset of the visual stimulus, we performed a timepoint-by-timepoint paired-samples *t* test between the 800 ms stimulus window and a concatenated baseline period of equal time and frequency parameters. To control for Type 1 error, a two-stage cluster and permutation testing approach similar to that described earlier (see the section titled "MEG Preprocessing, Time–Frequency Transformation, and Sensor-Level Statistics") was utilized, with specified criteria of at least 10,000 permutations and a threshold of $P < 0.01$.

Although phase coherence is relatively robust against amplitude effects compared to other measures of FC (e.g., traditional coherence), this still remains a concern. To account for this potential confound in our analyses, we correlated the baseline-corrected PLV of any significant increases or decreases in FC with the relative power at both of the relevant sources. Significant modulations of phase coherence that were found to significantly correlate with power at either source were not reported. However, as this approach is quite conservative, we did not exclude these instances of phase coherence from our behavioral correlations. Rather, for all behavioral correlations with FC, we computed the Pearson's partial correlation coefficient, within which we controlled for the variation accounted for by power at each of the relevant sources. To compute a partial correlation, two variables of interest are each regressed upon a third covariate, and the relationship between the residuals from these models is then computed using Pearson's product–moment coefficient. This essentially provides us with a correlation coefficient (and corresponding *P* value) that is corrected for any contributions made by the relative power at either source. For all partial correlations, we computed the average baseline-corrected FC value over the significant time-window per participant, and correlated this with relevant measures of behavior (i.e., RT and accuracy), while controlling for variance in the relative power of each of the functional sources averaged over the same significant time-window.

RESULTS

Behavioral Data

One participant was excluded from analysis due to equipment failure. Twenty-two participants (19 right-handed; 12 males) remained, all of whom were between the ages of 22 and 45 (mean = 32.73; SD = 7.24). As expected, all participants performed exceptionally well on the *VisAttend* task (Figure 1), with an average accuracy of 97.55% (range = 94–100%; SD = 1.90%). Response time (RT; time from stimulus onset to button-press) was more variable (mean = 576.10 ms; range = 451.33–802.86 ms; SD = 86.47 ms), and likely represents a more relevant measure of attention efficacy for this task. Neither RT nor accuracy was correlated with demographic measures (i.e., age, sex, and handedness).

Sensor-Level Data

To examine the frequency specificity of neural networks subserving the task, we first assessed oscillatory responses

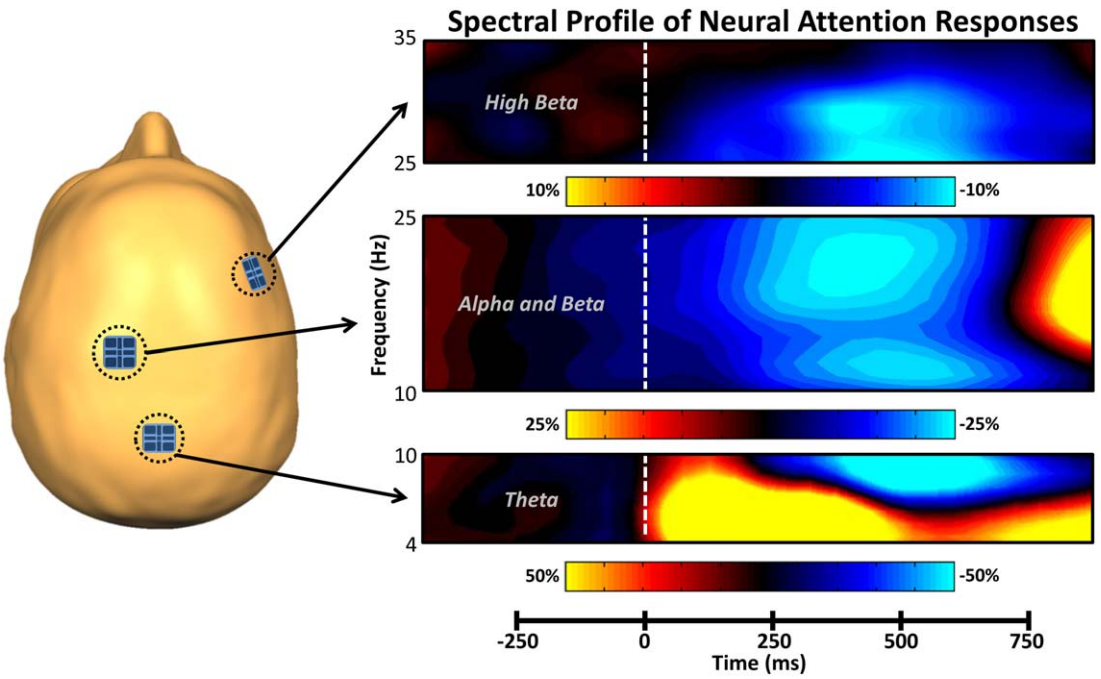

Figure 2.

Spectral time course of neural attention responses in the MEG sensor array. The schematic on the left indicates the spatial location of sensors of interest. On the right, time (in milliseconds) is denoted on the *x*-axis, with 0 ms defined as the onset of the stimulus grid, and frequency (in Hz) is shown on the *y*-axis. All signal power data are expressed as a percent difference from baseline (−460 to −60 ms), with each color legend underneath its respective spectrogram. All spectrograms represent group-averaged data from gradiometer sensors that were representative of the neural response in each region. The same sensors were selected in all participants and their approximate location relative to the head is shown on the left. As is apparent, theta activity in occipital regions strongly increased (i.e., synchronized) shortly after the onset of the stimulus, while alpha, beta, and high beta activity were all strongly decreased (i.e., desynchronized) over more anterior regions. Time–frequency windows with significant oscillatory activity (relative to baseline) were subjected to beamforming. [Color figure can be viewed at wileyonlinelibrary.com]

in the time–frequency domain. Analysis of the sensor-level spectrograms during visual processing revealed five frequency-specific oscillations (Figure 2). First, there was a large synchronization in the *theta* range (4–8 Hz) in a cluster of occipital sensors that stretched from 40 to 540 ms. This response largely overlapped in time with a desynchronization in the *beta* band (16–24 Hz; 40–440 ms) and a desynchronization in the *alpha* range (8–14 Hz; 190–540 ms), which were strongest in a cluster of sensors near the parietal cortices. The fourth significant response was a desynchronization in the *high beta* range (28–32 Hz) that emerged in a cluster of prefrontal sensors and lasted from 190 to 390 ms. Finally, there was a synchronization in the *gamma* range (54–86 Hz; 140–540 ms) in occipital sensors. To further facilitate mapping of the dynamic time course of these attention-related neural activations, the two most sustained responses (*theta* and *beta*) were each divided into two time windows of identical length and frequency range for subsequent source-localization analysis.

Source Imaging and Statistical Maps

Neural responses in the occipital cortices

To determine the spatial origin of the five sensor-level oscillations mentioned above, a beamformer was applied to the data of each participant (per time-frequency window). The output images were averaged across participants per time–frequency window, and three of these averages included bilateral peaks within the occipital cortices (Figure 3), including positive peaks in bilateral primary visual regions in the *theta* and *gamma* bands, as well as bilateral suppression in extrastriate visual regions in the *alpha* band.

Attention-network neural responses in the theta band

To identify regions outside the visual cortices that produced a significant response during the visuospatial task, we performed one-sample *t* tests on the beamformer images

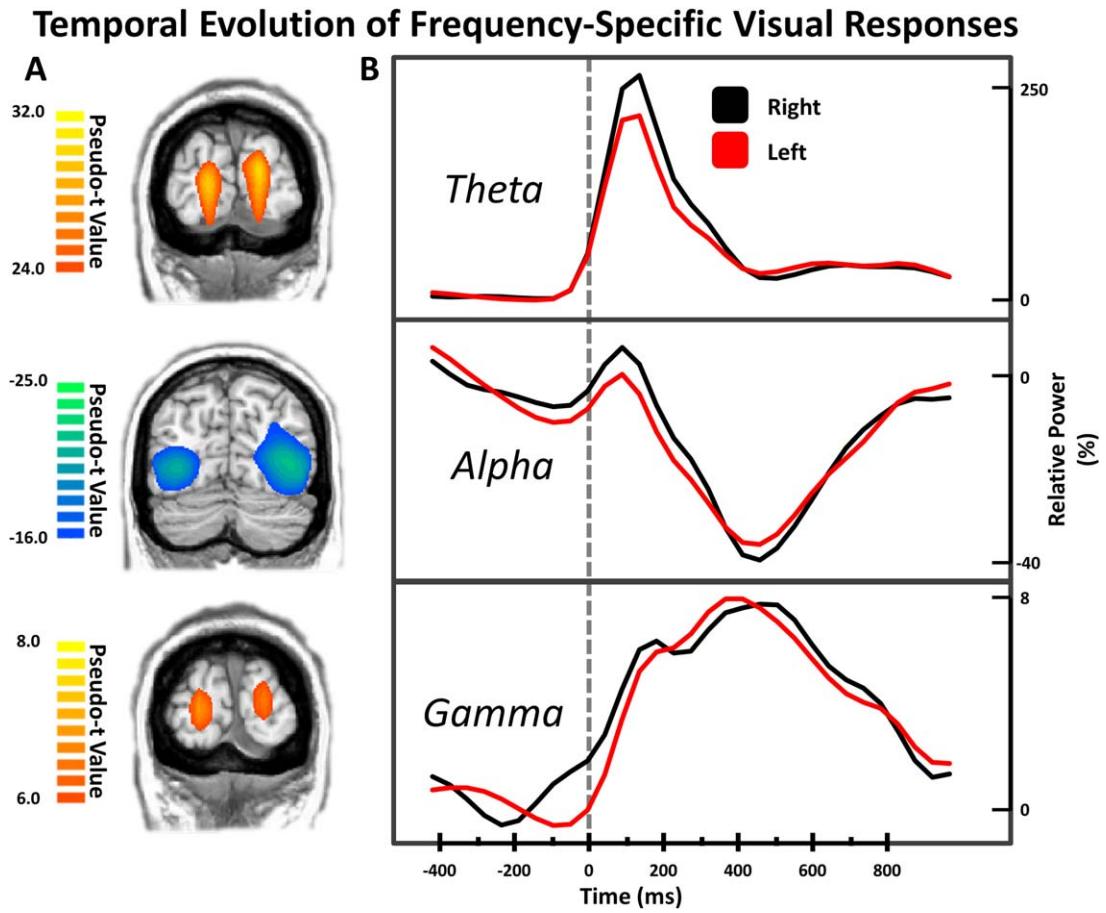

Figure 3.

Temporal evolution of frequency-specific visual responses. Coronal slices in (**A**) are group mean beamformer images of the bilateral visual responses at each frequency. The respective color legend for each image is displayed to the left. Hemisphere-specific peak voxel time series for each set of visual responses were extracted and are displayed in (**B**), with time (in milliseconds) denoted on the *x*-axis, and the respective percent-change in relative power for each plot denoted on the *y*-axis. As is apparent, the dynamic time course of the right (black) and left (red) visual cortices in each frequency range were very similar. [Color figure can be viewed at wileyonlinelibrary.com]

for each time–frequency window of interest. In the *theta* band, these responses were located almost exclusively in the frontal cortices (Figure 4A), and included significant peaks in the right inferior frontal cortex (RIFC), left dorsolateral prefrontal cortex (dlPFC), and premotor cortices during the early time window (40–290 ms; Figure 4A, upper panel). In the later time bin (290–540 ms; Figure 4A, lower panel), significant peaks emerged in the left inferior frontal cortex (LIFC), left PFC, left pre-supplementary motor area (pre-SMA), and left motor cortices.

Attention-network neural responses in the beta band

Similar to the *theta* responses, activity in the *beta* band was separated into two windows of equal duration prior to imaging. Unlike *theta* activity, responses in both of these windows originated from similar neuronal populations (Figure 4B, left), which included the bilateral superior parietal cortices (SPC), and left M1. In the *high beta* frequency band, the key brain regions were substantially different, and occurred only in the right hemisphere (Figure 4B, right). These included one peak in the RIFC, and a more substantial peak originating in the right anterior insula.

No significant peaks were observed outside of visual cortices in the *alpha* or *gamma* time–frequency windows of interest.

Functional Connectivity Analyses

Visuospatial attention dynamically modulates functional connectivity between homologous regions

The whole-brain statistical maps exhibited three sets of frequency-specific bilateral activations in homologous regions of the cortex, including the bilateral IFC in the *theta* band, the bilateral SPC in the *beta* band, and bilateral visual

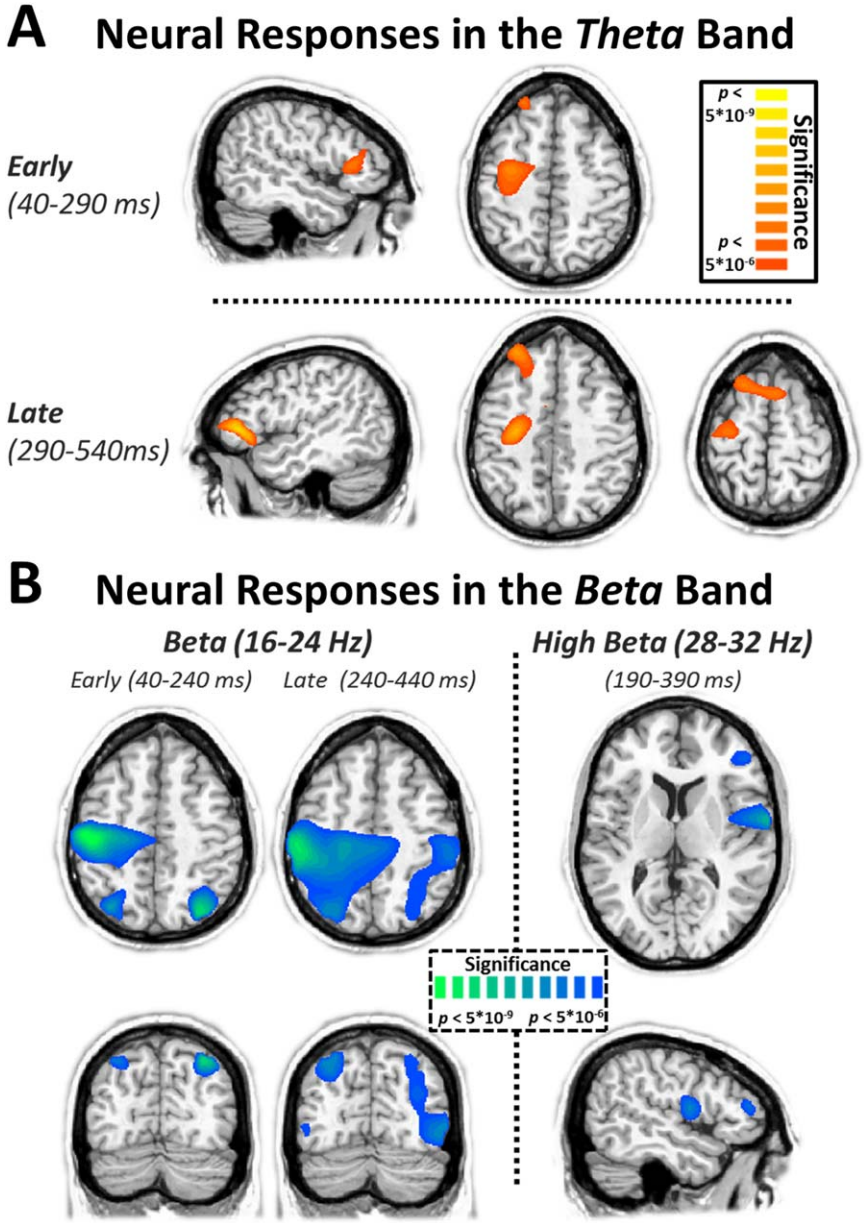

Figure 4.

Oscillatory neural responses in the *theta* and *beta* bands. (**A**) Attention to the visual stimuli elicited early responses (40–290 ms; top) in the right inferior frontal cortex (RIFC), left dorsolateral prefrontal cortex (dlPFC), and left primary motor cortex (M1) in the *theta* (4–8 Hz) band. Later responses (290–540 ms; bottom) in the *theta* band were centered on the left inferior frontal cortex (LIFC), the left dlPFC, the pre-supplementary motor area (pre-SMA), and the left M1. (**B**) Attending to the visual stimuli also elicited robust suppression of beta activity in the bilateral superior parietal cortices (SPC) and the left primary motor cortex (M1) in both the early and late time windows. In the *high beta* band, activity was centered on the right inferior frontal cortex (RIFC) and the right anterior insula during the 190–390 ms window. All images (statistical parametric maps) reflect one-sample *t* tests across all participants and have been thresholded at $P < 5 \times 10^{-6}$. The same significance thresholds were utilized on all statistical images throughout the analysis. [Color figure can be viewed at wileyonlinelibrary.com]

cortices in the *alpha* band. To examine whether dynamic FC between these regions was modulated as a function of attention allocation, we extracted the amplitude time series for each statistically defined peak, and estimated the phase-locking value (PLV) between each pair of homologous regions to create a dynamic FC time series for each

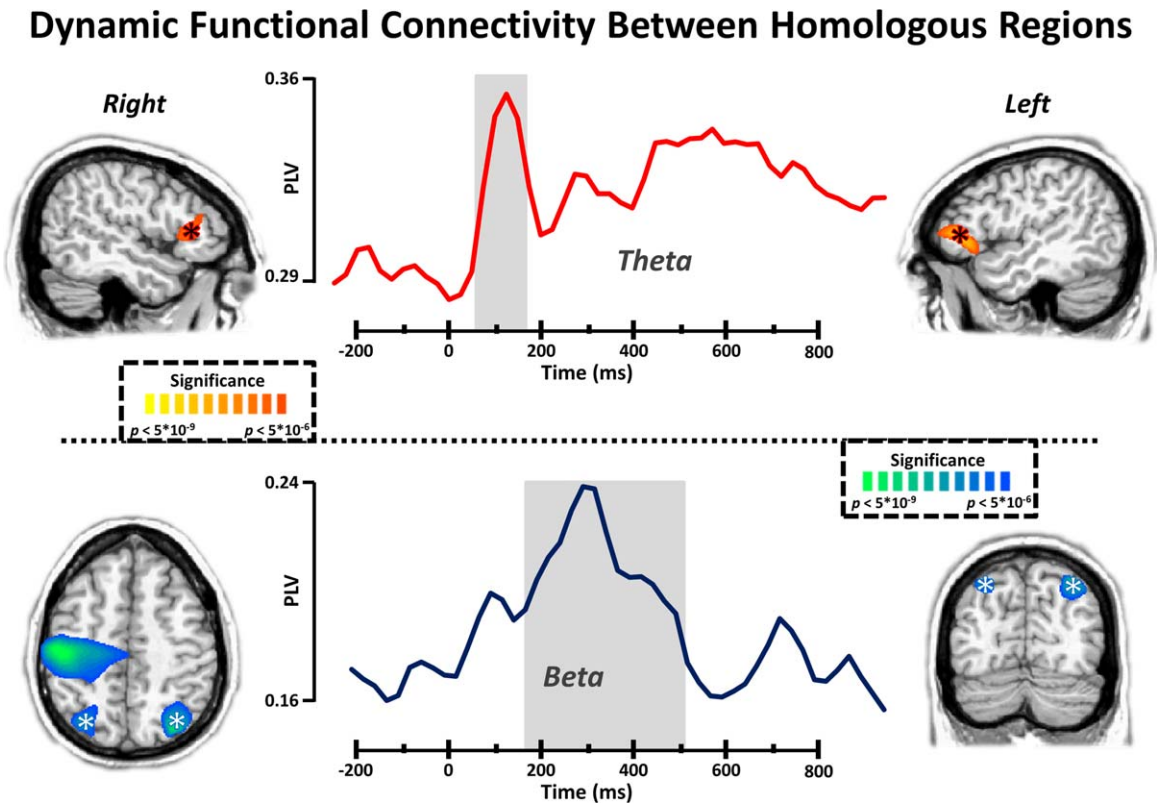

Figure 5.

Dynamic functional connectivity between homologous regions. Time series of dynamic functional connectivity between peak voxels in the bilateral inferior frontal cortices in the *theta* band (top) and bilateral superior parietal cortices in the *beta* band (bottom). Time (in milliseconds) is denoted on the *x*-axis and phase locking value (PLV) is denoted on the *y*-axis. Shaded regions indicate time windows of significant ($P < 0.01$, *corrected using permutation testing*) deviation from baseline. Asterisks reflect the bilateral sources between which connectivity was computed. All sources were extracted from the voxel with the highest *t* value within each of the clusters. [Color figure can be viewed at wileyonlinelibrary.com]

participant. These FC time series were then statistically tested against the baseline to uncover any significant modulations of FC following presentation of the visual stimulus. Of note, we excluded the *gamma* and *theta* V1 activations from this analysis, as the high spatial proximity of their bilateral peaks precluded any meaningful interpretation of their phase-locking [Lachaux et al., 1999].

We observed statistically significant transient increases in FC for the bilateral IFC and bilateral SPC regions (Figure 5), but not the visual cortices. Theta FC between the bilateral IFC increased significantly between 65 and 165 ms poststimulus onset ($P = 0.006$), and this increase peaked at 115 ms. Immediately following this increase in interhemispheric frontal FC in the *theta* band, bilateral SPC FC in the *beta* band sharply increased. This increase lasted from 165 to 465 ms poststimulus onset ($P < 0.001$), and reached a maxima at 290 ms. Neither of these significant modulations in FC showed a significant relationship with reaction time, or source amplitude, which can sometimes confound accurate FC measurements [Brookes et al., 2011].

Visuospatial attention dynamically modulates functional connectivity between frontal and visual cortices

Evidence for the influence of higher order "control" nodes on regions that process and integrate sensory information is abundant [Baldauf and Desimone, 2014; Buschman and Miller, 2007; He et al., 2007; Miller and Cohen, 2001; Szczepanski et al., 2014; Villalobos et al., 2005], particularly through FC in the lower frequency bands. We observed strong theta activity in response to our task in regions associated with top–down modulatory effects (i.e., the bilateral IFC and the left dlPFC), and in regions associated with visual processing (i.e., the primary visual cortices). Given this, we wanted to examine the dynamic modulation of FC between these bilateral frontal regions and the strongest peaks in the bilateral visual cortex following the presentation of the visual stimulus. To this end, we defined regional peaks using the statistical parametric maps. A transient increase in FC was observed between the

RIFC and the peak extracted from the left visual cortex, which lasted from 65 to 165 ms poststimulus onset, with a maxima at 140 ms ($P = 0.027$; Supporting Information, Figure S1). Dynamic modulation of FC was also observed at similar or later times between the left frontal sources and the visual cortices; however, in all these instances, relative power at the LIFC source was found to significantly correlate with baseline-corrected values of FC, and in the interest of caution, we examined these FC modulations only in subsequent correlation analyses within which we could control for this potential confound. These correlation analyses revealed an interesting relationship between frontovisual FC and performance on the visuospatial discrimination task. Dynamic increases in FC between the LIFC and bilateral visual cortices correlated strongly with decreased RT on the task (LIFC-LVis: $r = -0.501$, $P = 0.024$; LIFC-RVis: $r = -0.575$, $P = 0.008$). Furthermore, a dynamic increase in FC observed between the left dlPFC and RVis also correlated strongly with decreased RT ($r = -0.568$, $P = 0.009$). The dynamic increase in FC between the RIFC and the visual cortex did not exhibit a significant correlation with behavior, although a strong trend toward significance was present ($r = 0.420$, $P = 0.065$).

DISCUSSION

Herein, we examined the precise temporal progression of the frequency-specific neural responses that underlie visuospatial attention allocation, and the dynamic patterns of functional connectivity that subserve these networks. Unlike previous studies, we utilized a holistic and data-driven approach to determine the bandwidth and location of attention-related neural responses in distinct frequency ranges, and then characterized significant modulations in dynamic FC between these locations. As hypothesized, we observed significant neuronal activity in many regions of prototypical attention networks, and discovered that these responses were segregated not only by physical space across the brain but also by oscillatory frequency. Furthermore, we found that FC between these attention-network nodes was significantly modulated by increased allocation of attention to the visual space (i.e., as is necessary when making visuospatial determinations). We discuss the ramifications of our findings on current knowledge in the field, and the implications for future research, below.

The observed responses in visual cortex largely agree with previous literature on the oscillatory patterns that subserve visual and visuospatial attentional processing. The *theta* band response that we detected in bilateral striate cortex is often observed in evoked response studies, and the later decrease in alpha power in more lateral regions of the occipital lobes is a very common finding [Busch et al., 2004; Edden et al., 2009; Hari et al., 1997; Heinrichs-Graham and Wilson, 2015b; Hoogenboom et al., 2006; Makeig et al., 2002; Muthukumaraswamy and Singh, 2013; Vidal et al., 2006]. These neural responses are generally acknowledged as being initial sensory encoding (theta) and subsequent processing of the visual stimulus (alpha), respectively. We also observed a more prolonged increase in power in the *gamma* band, which originated in bilateral early visual cortices. Gamma responses to visual stimuli in the occipital cortices are a well-catalogued phenomenon, and are functionally segregated into stimulus feature encoding responses in V1 [Busch et al., 2004; Edden et al., 2009; Hoogenboom et al., 2006; Muthukumaraswamy and Singh, 2013; Vidal et al., 2006] and attention-modulated stimulus processing responses in extrastriate visual regions [Doesburg et al., 2008; Fries et al., 2001; Shibata et al., 1999; Tallon-Baudry et al., 2005; Vidal et al., 2006]. Our visual gamma findings fit nicely with these previous studies, and overall these data suggest that the processing of visuospatial stimuli in the occipital cortices is a complex, multicomponent series of distinct processes occurring at different oscillatory frequencies.

Beyond visual cortices, neural responses in the lowest frequency examined, *theta*, were primarily restricted to regions in the frontal cortices. In the earliest time window, significant activity was observed in the RIFC and left dlPFC, while in the late time window, significant activity emerged in the LIFC, left dlPFC, and pre-SMA. Since the advent of modern neuroimaging methods, the dlPFC has emerged as a major component in the top–down modulation of cognitive processes [MacDonald et al., 2000; Miller and Cohen, 2001], and receives direct input from a number of primary sensory regions, including visual cortex [Miller and Cohen, 2001]. This theory is supported by our finding that stronger coupling between the left dlPFC and visual cortex correlated strongly with reduced reaction time (i.e., better performance) on the task. Activation in the pre-SMA during attention tasks is also commonly reported, and has been associated with attention to response selection [Kennerley et al., 2004; Lau et al., 2004; Lawrence et al., 2003]. The timing of this response in our experiment (290–540 ms) supports this conclusion, as it directly preceded the mean RT (576.10 ms) for the task.

Based on recent literature, there are at least two possible roles for the inferior frontal cortical activity in this task. The more classical theory regarding the inferior frontal gyri postulates that the inferior frontal cortices (and particularly the RIFC) are important nodes in a system that functions to inhibit premature responses on behavioral tasks [Aron et al., 2004]. While possible, this particular function does not fit our visuospatial attention task especially well, as there was no prepotent response. Furthermore, more recent neuroimaging studies have provided evidence that these regions are a central component of a neural network serving the maintenance and online updating of behaviorally relevant task schemas, which of course would also include inhibiting prepotent responses [Hampshire et al., 2010; Verbruggen et al., 2010]. This theory integrates well with our findings, as the other components of this proposed network include the pre-SMA and the

posterior parietal cortex, both of which were significantly active during our attention task. Furthermore, the RIFC has been implicated as a likely convergence point between lower order right-lateralized "alerting" attention systems, and higher order bilateral "controlling" attention systems [Fox et al., 2006; He et al., 2007], while the LIFC has been more exclusively linked to "controlling" systems [He et al., 2007]. Together with these previous works, our results support the concept that the bilateral inferior frontal cortices are key players in a network that integrates task-relevant stimulus information, updates goal-driven schemas accordingly, and is involved in exerting subsequent top–down influences on other components of the visual stream. Under this theoretical framework, our FC findings in the *theta* band are particularly interesting. Theta-frequency oscillations are thought to play a critical role in the temporal organization of information transfer in the visual attention system [Busch et al., 2009; Landau and Fries, 2012], and we observed two distinct patterns of FC modulations in this band. The first was a transient increase in FC between bilateral IFC that began shortly after stimulus presentation, and had dissipated by around 200 ms after stimulus onset. Following the current framework, this dynamic connectivity may reflect the inferior frontal regions integrating current task-related developments with pre-established task-schema information prior to exerting any top–down modulatory control. Supporting this overall framework, increases in FC later in the time course between the (later-responding) LIFC and the visual cortices were found to correlate with reduced reaction time on the task. Intuitively, this makes sense as enhanced communication between the LIFC and early visual regions should lower the time necessary to produce a correct response.

In the *beta* band, we observed significant neural responses in the bilateral SPC and motor regions. Decreased beta power in M1 is often termed the motor-related event-related desynchronization, and has been observed in a number of tasks requiring a motor response [Cheyne et al., 2008; Jurkiewicz et al., 2006; Pfurtscheller and Lopes da Silva, 1999; Wilson et al., 2014]. The observed decrease in beta power in the bilateral SPC was especially interesting, as neural activity in these regions has been associated with visual attention for decades, and is commonly thought to facilitate attention shifts within the visual space [Corbetta et al., 1995; Lynch et al., 1977; Posner et al., 1984; Yantis et al., 2002]. Such shifts are thought to be supported by a saliency map [Bisley and Goldberg, 2010], whereby incoming visual representations are filtered through a precomposed set of attentional filters (i.e., top–down influences resultant of task instructions) and the most salient representation is selected for the allocation of attentional resources. Importantly, we observed that FC between the homologous SPC was strongly increased following presentation of the visual stimulus, peaking around 300 ms, and such FC between these regions has been found to be uniquely deficient in patients with hemispatial neglect [He et al., 2007]. Together, these findings suggest that parietal regions representing pertinent zones of attended visual space (e.g., the bilateral visual regions in our task) communicate dynamically, possibly to facilitate more rapid analysis of visual scenes while also maintaining high precision. Our *high-beta* band findings also agree with previous literature. As discussed earlier, the RIFC is an important component in the updating of relevant schematic constructs, and thus this decrease in high beta power in this location likely reflects reorienting toward the task demands. The anterior insula has also been implicated as a supporting node in task-relevant modulation of lower order attention regions, and the deployment of spatial attention [Eckert et al., 2009; Nelson et al., 2010].

Although our findings are novel and informative, it is important to acknowledge the limitations of our study. First, it is likely that the neuronal responses and interactions reported here represent only the most dominant patterns of oscillatory coding within this visuospatial attention-network, and further work will need to expand upon these findings using methodologies more sensitive to lower amplitude responses. Furthermore, due to the relatively low difficulty of this paradigm, we were unable to discern any interactions between dynamic modulations of FC and accuracy. It seems plausible that the correlations seen between the RIFC–LIFC connectivity and RT might have exhibited a reversed effect for accuracy, indicating a neural basis for the speed–accuracy tradeoff often seen on this type of task. Further experimentation is necessary to determine if this is the case.

Overall, our findings highlight the dynamic nature of information coding within the visuospatial attention system. The frequency specificity of neuronal responses in our task followed a general spatial parcellation, which indicates that information coding via oscillatory rhythms is regionally specialized within the visual attention circuit. Furthermore, FC between relevant nodes of this system were found to be dynamically modulated by the allocation of attention resources to the visual space, and some of these measures correlated strongly with measures of task performance. These findings emphasize the dynamic nature of long-range functional communication, both between homologous nodes and regulatory nodes in the human brain, which serves the rapid nature of visuospatial attention deployment and other essential cognitive faculties.

AUTHOR CONTRIBUTIONS

Conceptualization: TWW.
Methodology: TWW, AIW, EHG, and ALP.
Formal analysis: AIW, TJM, and TWW.
Resources: TWW.
Data curation: TWW.
Writing of the original manuscript: AIW.
Review and editing the manuscript: AIW, TWW, EHG, ALP, and TJM.

Visualization: AIW.
Supervision: TWW.
Funding acquisition: TWW.

ACKNOWLEDGMENTS

The funders had no role in study design, data collection and analysis, decision to publish, or preparation of the manuscript. The authors declare that they have no conflicts of interest with the content of this article.

REFERENCES

Aron AR, Robbins TW, Poldrack RA (2004): Inhibition and the right inferior frontal cortex. Trends Cogn Sci 8:170–177.

Baldauf D, Desimone R (2014): Neural mechanisms of object-based attention. Science 344:424–427.

Bingham C, Godfrey MD, Tukey JW (1967): Modern Techniques of Power Spectrum Estimation. IEEE Transactions on Audio and Electroacoustics. The Institute of Electrical and Electronics Engineers, Inc. pp 56–66.

Bisley JW, Goldberg ME (2010): Attention, intention, and priority in the parietal lobe. Annu Rev Neurosci 33:1–21.

Brookes MJ, Hale JR, Zumer JM, Stevenson CM, Francis ST, Barnes GR, Owen JP, Morris PG, Nagarajan SS (2011): Measuring functional connectivity using MEG: Methodology and comparison with fcMRI. NeuroImage 56:1082–1104.

Buchel C, Friston KJ (1997): Modulation of connectivity in visual pathways by attention: Cortical interactions evaluated with structural equation modelling and fMRI. Cereb Cortex 7:768–778.

Busch NA, Debener S, Kranczioch C, Engel AK, Herrmann CS (2004): Size matters: Effects of stimulus size, duration and eccentricity on the visual gamma-band response. Clin Neurophysiol 115:1810–1820.

Busch NA, Dubois J, VanRullen R (2009): The phase of ongoing EEG oscillations predicts visual perception. J Neurosci 29: 7869–7876.

Buschman TJ, Miller EK (2007): Top-down versus bottom-up control of attention in the prefrontal and posterior parietal cortices. Science 315:1860–1862.

Buzsaki G, Draguhn A (2004): Neuronal oscillations in cortical networks. Science 304:1926–1929.

Cheyne D, Bells S, Ferrari P, Gaetz W, Bostan AC (2008): Self-paced movements induce high-frequency gamma oscillations in primary motor cortex. NeuroImage 42:332–342.

Corbetta M, Shulman GL (2002): Control of goal-directed and stimulus-driven attention in the brain. Nat Rev Neurosci 3: 201–215.

Corbetta M, Shulman GL, Miezin FM, Petersen SE (1995): Superior parietal cortex activation during spatial attention shifts and visual feature conjunction. Science 270:802–805.

David O, Harrison L, Friston KJ (2005): Modelling event-related responses in the brain. NeuroImage 25:756–770.

Desimone R, Duncan J (1995): Neural mechanisms of selective visual attention. Annu Rev Neurosci 18:193–222.

Di Russo F, Martinez A, Hillyard SA (2003): Source analysis of event-related cortical activity during visuo-spatial attention. Cereb Cortex 13:486–499.

Doesburg SM, Roggeveen AB, Kitajo K, Ward LM (2008): Large-scale gamma-band phase synchronization and selective attention. Cereb Cortex 18:386–396.

Eckert MA, Menon V, Walczak A, Ahlstrom J, Denslow S, Horwitz A, Dubno JR (2009): At the heart of the ventral attention system: The right anterior insula. Hum Brain Mapp 30:2530–2541.

Edden RA, Muthukumaraswamy SD, Freeman TC, Singh KD (2009): Orientation discrimination performance is predicted by GABA concentration and gamma oscillation frequency in human primary visual cortex. J Neurosci 29:15721–15726.

Ernst MD (2004): Permutation methods: A basis for exact inference. Stat Sci 19:676–685.

Fox MD, Corbetta M, Snyder AZ, Vincent JL, Raichle ME (2006): Spontaneous neuronal activity distinguishes human dorsal and ventral attention systems. Proc Natl Acad Sci USA 103: 10046–10051.

Fries P, Reynolds JH, Rorie AE, Desimone R (2001): Modulation of oscillatory neuronal synchronization by selective visual attention. Science 291:1560–1563.

Gross J, Kujala J, Hamalainen M, Timmermann L, Schnitzler A, Salmelin R (2001): Dynamic imaging of coherent sources: Studying neural interactions in the human brain. Proc Natl Acad Sci USA 98:694–699.

Gross J, Schmitz F, Schnitzler I, Kessler K, Shapiro K, Hommel B, Schnitzler A (2004): Modulation of long-range neural synchrony reflects temporal limitations of visual attention in humans. Proc Natl Acad Sci USA 101:13050–13055.

Hampshire A, Chamberlain SR, Monti MM, Duncan J, Owen AM (2010): The role of the right inferior frontal gyrus: Inhibition and attentional control. NeuroImage 50:1313–1319.

Handel BF, Haarmeier T, Jensen O (2011): Alpha oscillations correlate with the successful inhibition of unattended stimuli. J Cogn Neurosci 23:2494–2502.

Hari R, Salmelin R (1997): Human cortical oscillations: A neuromagnetic view through the skull. Trends Neurosci 20:44–49.

Hari R, Salmelin R, Makela JP, Salenius S, Helle M (1997): Magnetoencephalographic cortical rhythms. Int J Psychophysiol 26: 51–62.

He BJ, Snyder AZ, Vincent JL, Epstein A, Shulman GL, Corbetta M (2007): Breakdown of functional connectivity in frontoparietal networks underlies behavioral deficits in spatial neglect. Neuron 53:905–918.

Heinrichs-Graham E, Wilson TW (2015a): Coding complexity in the human motor circuit. Hum Brain Mapp 36:5155–5167.

Heinrichs-Graham E, Wilson TW (2015b): Spatiotemporal oscillatory dynamics during the encoding and maintenance phases of a visual working memory task. Cortex 69:121–130.

Hoechstetter K, Bornfleth H, Weckesser D, Ille N, Berg P, Scherg M (2004): BESA source coherence: A new method to study cortical oscillatory coupling. Brain Topogr 16:233–238.

Honey CJ, Kötter R, Breakspear M, Sporns O (2007): Network structure of cerebral cortex shapes functional connectivity on multiple time scales. Proc Natl Acad Sci USA 104:10240–10245.

Hoogenboom N, Schoffelen JM, Oostenveld R, Parkes LM, Fries P (2006): Localizing human visual gamma-band activity in frequency, time and space. NeuroImage 29:764–773.

Jensen O, Gips B, Bergmann TO, Bonnefond M (2014): Temporal coding organized by coupled alpha and gamma oscillations prioritize visual processing. Trends Neurosci 37:357–369.

Jensen O, Tesche CD (2002): Frontal theta activity in humans increases with memory load in a working memory task. Eur J Neurosci 15:1395–1399.

Jurkiewicz MT, Gaetz WC, Bostan AC, Cheyne D (2006): Post-movement beta rebound is generated in motor cortex: Evidence from neuromagnetic recordings. NeuroImage 32:1281–1289.

Kennerley SW, Sakai K, Rushworth MF (2004): Organization of action sequences and the role of the pre-SMA. J Neurophysiol 91:978–993.

Lachaux JP, Rodriguez E, Martinerie J, Varela FJ (1999): Measuring phase synchrony in brain signals. Hum Brain Mapp 8:194–208.

Landau AN, Fries P (2012): Attention samples stimuli rhythmically. Curr Biol 22:1000–1004.

Landau AN, Schreyer HM, van Pelt S, Fries P (2015): Distributed attention is implemented through theta-rhythmic gamma modulation. Curr Biol 25:2332–2337.

Lau HC, Rogers RD, Haggard P, Passingham RE (2004): Attention to intention. Science 303:1208–1210.

Lawrence NS, Ross TJ, Hoffmann R, Garavan H, Stein EA (2003): Multiple neuronal networks mediate sustained attention. J Cogn Neurosci 15:1028–1038.

Lynch JC, Mountcastle VB, Talbot WH, Yin TC (1977): Parietal lobe mechanisms for directed visual attention. J Neurophysiol 40:362–389.

MacDonald AW, 3rd, Cohen JD, Stenger VA, Carter CS (2000): Dissociating the role of the dorsolateral prefrontal and anterior cingulate cortex in cognitive control. Science 288:1835–1838.

Makeig S, Westerfield M, Jung TP, Enghoff S, Townsend J, Courchesne E, Sejnowski TJ (2002): Dynamic brain sources of visual evoked responses. Science 295:690–694.

Maris E, Oostenveld R (2007): Nonparametric statistical testing of EEG- and MEG-data. J Neurosci Methods 164:177–190.

Marshall TR, O'Shea J, Jensen O, Bergmann TO (2015): Frontal eye fields control attentional modulation of alpha and gamma oscillations in contralateral occipitoparietal cortex. J Neurosci 35:1638–1647.

Miller EK, Cohen JD (2001): An integrative theory of prefrontal cortex function. Annu Rev Neurosci 24:167–202.

Muthukumaraswamy SD, Singh KD (2013): Visual gamma oscillations: The effects of stimulus type, visual field coverage and stimulus motion on MEG and EEG recordings. NeuroImage 69:223–230.

Nelson SM, Dosenbach NU, Cohen AL, Wheeler ME, Schlaggar BL, Petersen SE (2010): Role of the anterior insula in task-level control and focal attention. Brain Struct Funct 214:669–680.

Noesselt T, Hillyard SA, Woldorff MG, Schoenfeld A, Hagner T, Jancke L, Tempelmann C, Hinrichs H, Heinze HJ (2002): Delayed striate cortical activation during spatial attention. Neuron 35:575–587.

Papp N, Ktonas P (1977): Critical evaluation of complex demodulation techniques for the quantification of bioelectrical activity. Biomed Sci Instrum 13:135–145.

Pfurtscheller G, Lopes da Silva FH (1999): Event-related EEG/MEG synchronization and desynchronization: Basic principles. Clin Neurophysiol 110:1842–1857.

Posner MI, Petersen SE (1990): The attention system of the human brain. Annu Rev Neurosci 13:25–42.

Posner MI, Walker JA, Friedrich FJ, Rafal RD (1984): Effects of parietal injury on covert orienting of attention. J Neurosci 4: 1863–1874.

Rissman J, Gazzaley A, D'Esposito M (2004): Measuring functional connectivity during distinct stages of a cognitive task. NeuroImage 23:752–763.

Rosanova M, Casali A, Bellina V, Resta F, Mariotti M, Massimini M (2009): Natural frequencies of human corticothalamic circuits. J Neurosci 29:7679–7685.

Roux F, Uhlhaas PJ (2014): Working memory and neural oscillations: α-γ versus θ-γ codes for distinct WM information? Trends Cogn Sci 18:16–25.

Saalmann YB, Pigarev IN, Vidyasagar TR (2007): Neural mechanisms of visual attention: How top-down feedback highlights relevant locations. Science 316:1612–1615.

Schnitzler A, Gross J (2005): Normal and pathological oscillatory communication in the brain. Nat Rev Neurosci 6:285–296.

Shibata T, Shimoyama I, Ito T, Abla D, Iwasa H, Koseki K, Yamanouchi N, Sato T, Nakajima Y (1999): Attention changes the peak latency of the visual gamma-band oscillation of the EEG. Neuroreport 10:1167–1170.

Siegel M, Donner TH, Oostenveld R, Fries P, Engel AK (2008): Neuronal synchronization along the dorsal visual pathway reflects the focus of spatial attention. Neuron 60:709–719.

Spaak E, de Lange FP, Jensen O (2014): Local entrainment of alpha oscillations by visual stimuli causes cyclic modulation of perception. J Neurosci 34:3536–3544.

Szczepanski SM, Crone NE, Kuperman RA, Auguste KI, Parvizi J, Knight RT (2014): Dynamic changes in phase-amplitude coupling facilitate spatial attention control in fronto-parietal cortex. PLoS Biol 12:e1001936.

Tallon-Baudry C, Bertrand O, Henaff MA, Isnard J, Fischer C (2005): Attention modulates gamma-band oscillations differently in the human lateral occipital cortex and fusiform gyrus. Cereb Cortex 15:654–662.

Taulu S, Simola J (2006): Spatiotemporal signal space separation method for rejecting nearby interference in MEG measurements. Phys Med Biol 51:1759–1768.

Uusitalo MA, Ilmoniemi RJ (1997): Signal-space projection method for separating MEG or EEG into components. Med Biol Eng Comput 35:135–140.

Valencia M, Martinerie J, Dupont S, Chavez M (2008): Dynamic small-world behavior in functional brain networks unveiled by an event-related networks approach. Phys Rev E Stat Nonlin Soft Matter Phys 77:050905.

Verbruggen F, Aron AR, Stevens MA, Chambers CD (2010): Theta burst stimulation dissociates attention and action updating in human inferior frontal cortex. Proc Natl Acad Sci USA 107: 13966–13971.

Vidal JR, Chaumon M, O'Regan JK, Tallon-Baudry C (2006): Visual grouping and the focusing of attention induce gamma-band oscillations at different frequencies in human magnetoencephalogram signals. J Cogn Neurosci 18:1850–1862.

Villalobos ME, Mizuno A, Dahl BC, Kemmotsu N, Muller RA (2005): Reduced functional connectivity between V1 and inferior frontal cortex associated with visuomotor performance in autism. NeuroImage 25:916–925.

Wiesman AI, Heinrichs-Graham E, Coolidge NM, Gehringer JE, Kurz MJ, Wilson TW (2017): Oscillatory dynamics and functional connectivity during gating of primary somatosensory responses. J Physiol. 595:1365–1375.

Wiesman AI, Heinrichs-Graham E, McDermott TJ, Santamaria PM, Gendelman HE, Wilson TW (2016): Quiet connections: Reduced fronto-temporal connectivity in nondemented Parkinson's Disease during working memory encoding. Hum Brain Mapp 37:3224–3235.

Wilson TW, Heinrichs-Graham E, Becker KM (2014): Circadian modulation of motor-related beta oscillatory responses. NeuroImage 102 Pt 2:531–539.

Yantis S, Schwarzbach J, Serences JT, Carlson RL, Steinmetz MA, Pekar JJ, Courtney SM (2002): Transient neural activity in human parietal cortex during spatial attention shifts. Nat Neurosci 5:995–1002.